

Hyperfine tensors of nitrogen-vacancy center in diamond from *ab initio* calculations

Adam Gali^{1,2}

¹*Department of Atomic Physics, Budapest University of Technology and Economics, Budafoki út 8., H-1111, Budapest, Hungary*

²*Department of Physics and School of Engineering and Applied Sciences,
Harvard University, Cambridge, Massachusetts 02138, USA*

We determine and analyze the charge and spin density distributions of nitrogen-vacancy (N-V) center in diamond for both the ground and excited states by *ab initio* supercell calculations. We show that the hyperfine tensor of ^{15}N nuclear spin is negative and strongly anisotropic in the excited state, in contrast to previous models used extensively to explain electron spin resonance measurements. In addition, we detect a significant redistribution of the spin density due to excitation that has serious implications for the quantum register applications of N-V center.

Nitrogen-vacancy (N-V) centers in diamond have numerous peculiar properties that make them a very attractive solid state system for fundamental investigations of spin based phenomena. Recently, this defect has been proposed for several applications, like quantum information processing [1, 2, 3, 4], ultrasensitive magnetometer [5, 6], and measurement of zero-point fluctuations or preparing quantum-correlated spin-states over macroscopic distance [7]. In these measurements, a room temperature read-out of *single nuclear spins* in diamond has been achieved by coherently mapping nuclear spin states onto the electron spin of a single N-V center [3, 8] which can be *optically* polarized and read out with long coherence time [9, 10]. Particularly, this has been the basis in realization of a nuclear-spin-based quantum register [11] and multipartite entanglement among single spins at room temperature [12]. The polarization of a single nuclear spin has been achieved by using either a combination of selective microwave excitation and controlled Larmor precession of the nuclear-spin state [11] or a level anticrossing *in the excited state* [13]. Understanding the spin states and levels is of critical importance for optical control of N-V centers in both the ground and excited states. Especially, the hyperfine interaction couples the electron spin and nuclear spin, thus determination of hyperfine tensors of the nuclei with non-zero nuclear spin plays a key role both in creation of entanglement states and in the decoherence process [3, 14].

Recently, the hyperfine signals in the ground [13, 15] and excited [16] states have been detected in N-V centers but with contradicting interpretations. In a conventional electron paramagnetic resonance (EPR) spectrum on the ensemble of N-V centers, the ^{15}N signal was assumed to be *positive* with slight anisotropy in the ground state while Fuchs *et al.* and Jacques *et al.* assumed an isotropic *negative* hyperfine constant for ^{15}N in the ground state [13, 16] based on previous EPR and optically detected magnetic resonance (ODMR) measurements [17, 18]. Recently, Fuchs *et al.* have reported that the hyperfine splitting of ^{15}N should be $\sim 20\times$ larger in the excited state than in the ground state [16]. The excited-state ^{15}N hyperfine signal was assumed to be isotropic in their model [16]. While we already addressed the hyperfine tensor of ^{14}N in the ground state [19], the lack of the detailed study on ^{15}N hyperfine signal and the proximate ^{13}C isotopes *both* in the ground and excited states prohibits the understanding of

the intriguing physical properties of this defect. In this Letter, we thoroughly investigate the hyperfine tensors of proximate ^{15}N and ^{13}C isotopes of the N-V center *both* in the ground and excited states by means of high level *ab initio* supercell all-electron plane wave calculations. In addition, we analyse the overall charge and spin density distributions before and after the optical excitation. We show that the hyperfine constants of ^{15}N is *positive* and possibly slightly anisotropic in the ground state while *negative* and *strongly anisotropic* in the excited state. In addition, the hyperfine splittings of the proximate ^{13}C isotopes change also significantly that has serious implications both in the interpretation of the excited-state spectroscopy signals and in the quantum-information applications.

The negatively charged NV-center in diamond [20] consists of a substitutional nitrogen atom associated with a vacancy at an adjacent lattice site (Fig. 1a). The ground state has 3A_2 symmetry where one a_1 defect level in the gap is fully occupied by electrons while the double degenerate e -level above that is occupied by only two electrons with parallel alignment of spins (Fig. 1b). Thus, this defect has $S=1$ high spin ground state [21]. By promotion one electron from the a_1 -level to the e -level will result in the excited 3E state. Both states can be described by conventional density functional methods. The ground state can be readily described by spin density functional theory while the excited state can be obtained by constrained occupation of states [19]. We optimized the geometry for both the ground and excited states, and calculated the charge and spin densities at the optimized geometries.

We applied the PBE functional [24] to calculate the spin density of the defect. First, the diamond primitive lattice was optimized, then a simple cubic 512-atom supercell was constructed from that. Finally, we placed the negatively charged NV-defect into the supercell, and optimized under the given electronic configuration. We utilized the VASP code for geometry optimization [25]. We applied plane wave basis set (cut-off: 420 eV) with PAW-method [26]. During the optimization of the lattice constant we applied twice as high plane wave cut-off and 12^3 Monkhorst-Pack K-point set [27]. For the 512-atom supercell we used the Γ -point that provided convergent charge density. We plugged the optimized geometry into the CPPAW supercell plane wave code with PAW-method that provides the hyperfine tensors [28]. We applied

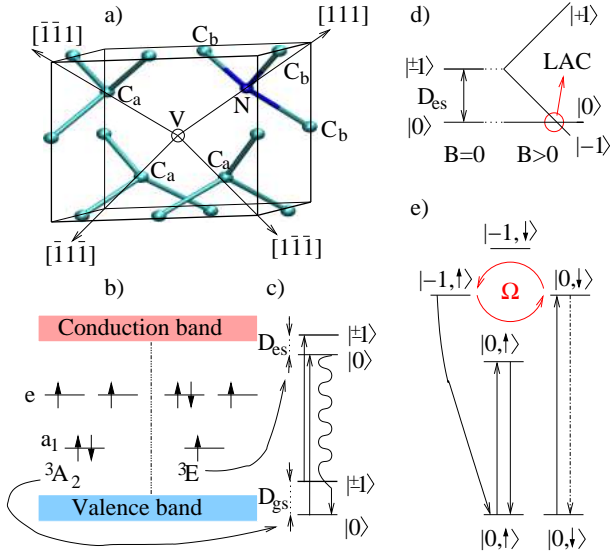


FIG. 1: (Color online) a) The structure of nitrogen-vacancy (N-V) defect in our particular working frame. The place of vacancy is denoted by an empty circle. b) The schematic single particle picture of the $m_s = 1$ high spin states in ground state ($^3A_{2,gs}$) and excited state ($^3E_{es}$). c) The fine structure of the 3A_2 and 3E states at room temperature due to spin-spin interaction. Zero-field splittings are $D_{gs}=2.88$ GHz [22], $D_{gs}=1.42$ GHz [23]. During optical excitations the fluorescence is predominantly active for the $m_s = 0$ ground state ($|0\rangle$) due to a non-radiative intersystem crossing of the $|\pm 1\rangle$ es states with the many-body singlet states (not shown here). d) Splittings of the es substates in the presence of the magnetic field (B). LAC is expected between $|0\rangle$ and $|-1\rangle$ states. e) Simplified energy-level diagram with including the hyperfine structure associated with ^{15}N nuclear spin states $|\uparrow\rangle$ and $|\downarrow\rangle$ in the case of LAC regime of the applied B-field. At LAC, precession frequency Ω between excited-state sublevels $|0, \downarrow\rangle$ and $|-1, \uparrow\rangle$ can lead to nuclear-spin flip, which can be transferred to the ground state through non-radiative intersystem crossing (curved arrow).

the same basis set and projectors in both codes yielding virtually equivalent spin density of the defects. Other technical details are given in Ref. 19. The charge density distribution was analyzed by the Bader-method [29]. We briefly mention here that we provide the principal values of the hyperfine tensors, called, A_{11} , A_{22} , and A_{33} that can be found by diagonalization of the hyperfine tensors. If the hyperfine field has C_{3v} symmetry then $A_{11}=A_{22}=A_{\perp}$ and $A_{33}=A_{\parallel}$ where \parallel means that hyperfine field coincides with the symmetry axis of the defect. The Fermi-contact term (a) is defined as $a = (A_{\parallel} + 2A_{\perp})/3$ while the dipole-dipole term (b) as $b = (A_{\parallel} - A_{\perp})/3$. The hyperfine field is isotropic when $b = 0$, i.e., $A_{\perp}=A_{\parallel}$.

First, we discuss the geometry of the defect. The obtained distance between the carbon atoms is 1.54 \AA in perfect diamond. In the nitrogen-vacancy defect there are three carbon atoms (C_a) and one nitrogen atom (N) closest to the vacant site each possessing a dangling bond (Fig. 1a). The defect conserves its C_{3v} symmetry during the outward relaxation, and the dangling bonds of the C_a and N atoms will point to

the vacant site. The symmetry axis will go through the vacant site and the N-atom which is the $[111]$ direction in our particular working frame (see Fig. 1a). We found in our PBE calculations that the C_a atoms are closer to the vacant site (1.64 \AA) than the N-atom (1.69 \AA) in the ground state. We obtained $5.97e$ Bader-charge on the N-atom that it is $0.97e$ larger than the number of valence electrons of the neutral N-atom. N-atom is more electro-negative than the C-atom. Indeed, the three C-atoms bound to N-atom (C_b) have $3.69e$ Bader-charge, so there is significant charge transfer from C_b atoms toward the N-atom ($\sim 0.93e$ as total). That is the main source of the negative polarization of the N-atom. We found that the negative charge is distributed on many atoms around the defect. The C_a atoms are even slightly positively polarized ($3.97e$) that will finally induce a dipole moment in the defect. Next, we briefly discuss the spin density of the ground state. The spin density is primarily originated from the unpaired electrons on the e defect level in the gap. Due to symmetry reasons [19, 30] the e -level is only localized on the C_a atoms but *not* on the N-atom. Therefore, large spin density is expected on the C_a atoms while negligible on the N-atom. Indeed, very small hyperfine splitting was found for ^{14}N [17] and ^{15}N [15, 18]. However, the sign of the Fermi-contact term of the hyperfine interaction for ^{15}N was contradictory. Rabreau *et al.* assumed a negative value [18] while Felton *et al.* has recently proposed a positive value [15]. The gyromagnetic factor of ^{15}N (γ_N) is negative, thus negative(positive) Fermi-contact hyperfine value (a) indicates positive(negative) spin density on the N-atom (n_s) because $a \sim \gamma_N n_s$. In our previous LDA calculation [19] we detected negative spin density on N-atom. Our improved PBE calculation justifies this scenario. Due to symmetry reasons the direct spin polarization of N-atom does not occur in the ground state but the large spin density on the C_a atoms can polarize the core electrons of the N-atom, i.e., it is an indirect and weak spin polarization. In our PBE calculation we can also detect a slight dipole-dipole interaction for ^{15}N which is outside of our error bar ($\sim 0.3 \text{ MHz}$ [19]). Our conclusions agree with the findings of Felton *et al.* [15]: the ^{15}N has *positive* hyperfine splittings and it is slightly anisotropic (see Table I). The calculated hyperfine tensors for C_a atoms agree nicely with the recent experimental values recorded at low temperature [15]. The fair qualitative agreement between the experiment and theory for the ground state allows us to study the less known excited state with our tools.

In the excited state we found a significant re-arrangement of atoms compared to the ground state. The C_a atoms now farther from the vacant site (1.70 \AA) than the N-atom (1.63 \AA) in contrast to the case of the ground state. The N-atom attracts less electrons from its neighbor C-atoms: the Bader-charge of N-atom ($5.88e$) is $0.09e$ less than in the ground state. Consequently, the Bader-charge of C_b atoms increases by $0.03e$. It is important to note that the Bader-charge of C_a atoms increases from $3.97e$ to $4.04e$. Thus, the excitation induces a change in the dipole moment of the defect. Next, we discuss the change in the spin density distribution upon excitation. Fig. 2 shows

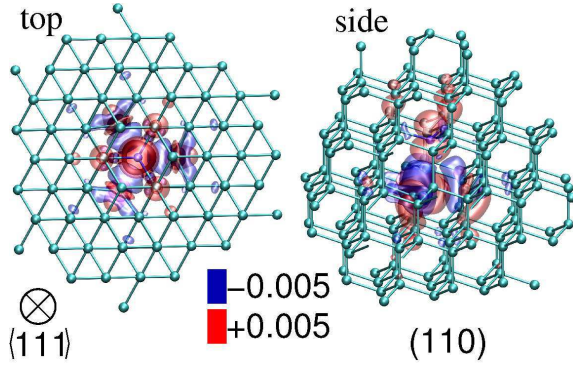


FIG. 2: (Color online) The calculated spin density difference between the excited 3E and the ground 3A_2 states of the NV center. We chose two representative isosurface values indicated in the colored rectangles. The blue(cyan) ball(s) represent the nitrogen(carbon) atoms. The vacant site is below the nitrogen atom.

TABLE I: 3A_2 ground state (rows 2,3) versus 3E excited state (rows 4,5). The calculated principal values of the hyperfine tensor (columns 2 to 4) compared to the known experimental data (columns 5 to 7) in MHz. The experimental data on ${}^{15}\text{N}$ is taken from Refs. 15, 16. See text for the meaning of the question mark.

Atom	A_{11}	A_{22}	A_{33}	A_{11}^{exp}	A_{22}^{exp}	A_{33}^{exp}
${}^{15}\text{N}$	2.7	2.7	2.3	3.65(3)	3.65(3)	3.03(3)
${}^{13}\text{C}(3\times)$	119.7	120.4	201.1	121.1(1)	121.1(1)	199.21(1)
${}^{15}\text{N}$	-39.2	-39.2	-57.8	?	?	61 ± 6
${}^{13}\text{C}(3\times)$	56.7	56.7	126.0			

the calculated difference of the spin densities in the excited and ground states. As one can see that the spin density enhanced a lot around N-atom (indicating with red lobes) while it dropped around the C_a atoms (indicating with blue lobes). This can be explained by the hole left on the a_1 defect level in the gap after excitation. The a_1 defect level is significantly localized on the N-atom [19]. Thus, the spin polarization of the a_1 defect level will spin polarize the N-atom considerably. Consequently, the spin polarization of the C_a atoms will be smaller. According to the calculations the hyperfine constants of ${}^{13}\text{C}$ isotopes are dropped by around 50% (see Table I). However, the overall magnetization density of the N and C_a atoms is about 95% the same *both* in the ground and excited states. In other words, the spin density mostly redistributed between the N-atom and the three C_a -atoms upon excitation. Indeed, it has been very recently found by using excited state spectroscopy in ${}^{15}\text{N}$ enriched diamond samples that the ${}^{15}\text{N}$ hyperfine signal is ≈ 20 times larger (~ 60 MHz) in the excited state than in the ground state [16]. Our calculations can explain this feature. However, the applied model Hamiltonian for describing the EPR of ${}^{15}\text{N}$ hyperfine signal ($A^{(\text{N})}$) was incomplete in Refs. 13, 16. Fuchs *et al.* and Jacques *et al.* studied individual NV centers by confocal photoluminescence microscopy where the actual defect was aligned to the [111] axis and the applied magnetic field was parallel to this

axis, thus the angular dependence of $A^{(\text{N})}$ was not measured. They assumed isotropic $A^{(\text{N})}$ for the excited state while our study shows that it is strongly anisotropic. Fuchs *et al.* also noticed that $A^{(\text{N})}$ should have the opposite sign in the ground and excited states [16]. Our study shows that $A^{(\text{N})}$ is positive(negative) in the ground(excited) states in contrast to the previous assumptions [13, 16].

Now, we discuss the consequence of our findings in the light of recent experiments on the dynamic polarization of single nuclear spins of the NV center [13, 16]. It has been demonstrated that the effective nuclear-spin temperature corresponds to a μK in this process [13] *decoupled* from the ambient temperature that can be the basic physical process in the measurement of zero-point fluctuations [7]. In these measurements the de-polarization of the nuclear spins of ${}^{15}\text{N}$ [13, 16] and ${}^{13}\text{C}_a$ [13] have been demonstrated. This has been achieved by the level anticrossing (LAC) of the electron spin m_s sublevels in the excited state. The LAC effect may appear if the m_s sublevels cross at a given external magnetic field (see Fig. 1c,d). We show a refined and corrected model of Ref. 13 accounted for LAC. We study the de-polarization of ${}^{15}\text{N}$ isotope but it can be generalized for the ${}^{13}\text{C}$ isotopes straightforwardly. The Hamiltonian of the system (with neglecting the nuclear-Zeeman splitting) can be written as [13],

$$H = D_{\text{es}} \hat{S}_z^2 + g_e \mu_B B \hat{S}_z + A_{\text{es}} \hat{S} \hat{I}, \quad (1)$$

where \hat{S} and \hat{I} are the electron and nuclear-spin operators, D_{es} the excited-state zero-field splitting, g_e the electron g factor, μ_B the Bohr-magneton, and A_{es} the excited hyperfine coupling. We assume positive B -field. Because A_{es} is anisotropic, the $A_{\text{es}} \hat{S} \hat{I}$ term can be written with the a_{es} and b_{es} hyperfine splittings and the spin-shift operators as,

$$\frac{\hat{S}_+ \hat{I}_- + \hat{S}_- \hat{I}_+}{2} (a_{\text{es}} - b_{\text{es}}) + \hat{S}_z \hat{I}_z (a_{\text{es}} + 2b_{\text{es}}) \quad (2)$$

The hyperfine field of ${}^{15}\text{N}$ is parallel to the symmetry axis, and $(a_{\text{es}} - b_{\text{es}}) = A_{\perp} \approx -39$ MHz while $(a_{\text{es}} + 2b_{\text{es}}) = A_{\parallel} \approx -58$ MHz. According to a recent study [23] $D_{\text{es}} = +1.42$ GHz ($m_s = 0$ sublevel is below $m_s = \pm 1$ sublevels), so we can restrict our study to the excited state $m_s = 0$ and $m_s = -1$ sublevels (see Fig. 1d). In the basis $[|-1, \downarrow\rangle; |-1, \uparrow\rangle; |0, \downarrow\rangle; |0, \uparrow\rangle]$ and by choosing the origin of energy level at level $|0, \uparrow\rangle$, the Hamiltonian described by Eqs. 1,2 can be written as

$$H = \begin{pmatrix} \mathcal{E}_{-1}^{\downarrow} - c & 0 & 0 & 0 \\ 0 & \mathcal{E}_{-1}^{\uparrow} - c & d & 0 \\ 0 & d & 0 & 0 \\ 0 & 0 & 0 & 0 \end{pmatrix}; \quad \begin{cases} \mathcal{E}_{-1}^{\uparrow} = D_{\text{es}} \pm A_{\parallel}/2 \\ c = g_e \mu_B B \\ d = A_{\perp}/\sqrt{2} \end{cases}.$$

The eigenstates of this Hamiltonian are $|0, \uparrow\rangle$, $|-1, \downarrow\rangle$, $|+\rangle = \alpha|0, \downarrow\rangle + \beta|-1, \uparrow\rangle$ and $|-\rangle = \beta|0, \downarrow\rangle - \alpha|-1, \uparrow\rangle$. By following the arguments in Ref. 13, the transition from the ground state $|0, \uparrow\rangle$ to the excited state remains nuclear spin conserving, whereas the transition from $|0, \downarrow\rangle$ results in $(\alpha|+\rangle + \beta|-\rangle)$ in the excited state (see Fig. 1e). This superposition state then starts to precess between the appropriate states at frequency $\Omega = 1/(2\hbar) \times [(\mathcal{E}_{-1}^{\uparrow} - c)^2 + 4d^2]^{1/2}$,

where \hbar is Planck's constant. The precession frequency depends on B via electron Zeeman-effect (c in our notation) that is minimal at LAC resonance, and will be equal to $|d|/\hbar = |A_{\perp}|/\sqrt{2}\hbar$. Jacques *et al.* assumed isotropic hyperfine splitting for ^{15}N , therefore, they applied ≈ 60 MHz in this formula [13]. Our analysis shows that rather the $|A_{\perp}| \approx 39$ MHz should be substituted here. Nevertheless, this precession frequency is still at the same order of magnitude as the excited state decay rate, 12 ns [16]. Thus, the spin-flip process is very efficient between $|0, \downarrow\rangle$ and $|-1, \uparrow\rangle$ states, and we can explain the de-polarization of ^{15}N found in the experiments [10, 13, 16]. It has been found that the probability of the de-polarization effect significantly depends on the misalignment of the magnetic field from the symmetry axis [13]. This may be partially explained by the anisotropy of the ^{15}N hyperfine splitting beside the mixing of the spin states.

We found other intriguing properties of the spin density in the excited state. As apparent in Fig. 2, the spin density and the corresponding hyperfine tensors change considerably also for the proximate ^{13}C isotopes. We show the hyperfine tensors only for the most significant change, for C_a atoms in Table I. Beside that new ^{13}C isotope becomes active above N-atom that has negligible spin density in the ground state. In addition, the spin density of the sets of 6(3) C-atoms at $R=3.9$ Å decreases(increases) due to excitation where R is the distance from the vacant site. According to our previous study [19], one of these ^{13}C isotopes was manipulated in the qubit and quantum register applications [3, 11]. Our study shows that during the optical set and read-out processes the spin-density of the addressed proximate ^{13}C isotopes changes indicating an effective oscillating magnetic field with the inverse lifetime of the excited-state. This may also influence the decoherence of the entangled electron-nuclear spin state that has not yet been considered [14].

AG acknowledges support from Hungarian OTKA No. K-67886. The fruitful discussion with Jeronimo Maze is appreciated.

- [2] R. J. Epstein, F. Mendoza, Y. K. Kato, and D. D. Awschalom, *Nat. Phys.* **1**, 94 (2005).
- [3] L. Childress *et al.*, *Science* **314**, 281 (2006).
- [4] R. Hanson *et al.*, *Science* **320**, 352 (2008).
- [5] J. R. Maze *et al.*, *Nature* **455**, 644 (2008).
- [6] G. Balasubramanian *et al.*, *Nature* **455**, 648 (2008).
- [7] J. Wrachtrup, *Nature Physics* **5**, 248 (2009).
- [8] F. Jelezko *et al.*, *Phys. Rev. Lett.* **93**, 130501 (2004).
- [9] F. Jelezko *et al.*, *Phys. Rev. Lett.* **92**, 076401 (2004).
- [10] T. Gaebel *et al.*, *Nature Physics* **2**, 408 (2006).
- [11] M. V. Gurudev Dutt *et al.*, *Science* **316**, 312 (2007).
- [12] P. Neumann *et al.*, *Science* **320**, 1326 (2008).
- [13] V. Jacques *et al.*, *Phys. Rev. Lett.* **102**, 057403 (2009).
- [14] J. R. Maze, J. M. Taylor, and M. D. Lukin, *Phys. Rev. B* **78**, 094303 (2008).
- [15] S. Felton *et al.*, *Phys. Rev. B* **79**, 075203 (2009).
- [16] G. D. Fuchs *et al.*, *Phys. Rev. Lett.* **101**, 117601 (2008).
- [17] X.-F. He, N. B. Manson, and P. T. H. Fisk, *Phys. Rev. B* **47**, 8816 (1993).
- [18] J. R. Rabeau *et al.*, *Applied Physics Letters* **88**, 023113 (2006).
- [19] A. Gali, M. Fyta, and E. Kaxiras, *Phys. Rev. B* **77**, 155206 (2008).
- [20] G. Davies and M. F. Hamer, *Proc. R. Soc. London Ser. A* **348**, 285 (1976).
- [21] J. P. Goss *et al.*, *Phys. Rev. Lett.* **77**, 3041 (1996).
- [22] J. H. N. Loubser and J. P. van Wyk, in *Diamond Research (London)* (Industrial Diamond information Bureau, London, 1977), pp. 11–15.
- [23] A. Batalov *et al.*, arXiv:0902.2330, 2009.
- [24] J. P. Perdew, K. Burke, and M. Ernzerhof, *Phys. Rev. Lett.* **77**, 3865 (1996).
- [25] G. Kresse and J. Furthmüller, *Phys. Rev. B* **54**, 11169 (1996).
- [26] P. E. Blöchl, *Phys. Rev. B* **50**, 17953 (1994).
- [27] H. J. Monkhorst and J. K. Pack, *Phys. Rev. B* **13**, 5188 (1976).
- [28] P. E. Blöchl, C. J. Först, and J. Schimpl, *Bull. Mater. Sci.* **26**, s33 (2001).
- [29] W. Tang, E. Sanville, and G. Henkelman, *J. Phys.: Condens. Matter* **21**, 084204 (7pp) (2009).
- [30] A. Lenef and S. C. Rand, *Phys. Rev. B* **53**, 13441 (1996).

[1] A. Gruber *et al.*, *Science* **276**, 2012 (1997).